Peer-reviewed version available at *Biofuels* **2020**; doi:10.1080/17597269.2020.1759179

Experimental study and validation of a kinetic scheme for Hydrothermal Carbonization reactions

Fidel Vallejo, Luis A. Diaz-Robles, Jorge Poblete, Francisco Cubillos*

Departamento de Ingeniería Química, Universidad de Santiago de Chile, Libertador Bernardo O'Higgins 3363, Estación Central, Chile

Programa Centro de Valorización de Residuos y Economía Circular, Chile

* fidel.vallejo@usach.cl - https://orcid.org/0000-0001-5835-298X

Acknowledgments

This work has been founded by Projects FONDEF ID18I10182 and BMBF-CONICYT 150067.

F. Vallejo acknowledges the support of the Conicyt National Doctorate Grant Folio 21170340.

Experimental study and validation of a kinetic scheme for Hydrothermal Carbonization reactions

Abstract

This study presents a new kinetic scheme for the mass yield prediction of waste lignocellulosic biomasses treated by Hydrothermal Carbonization (HTC). The proposed reactions are based on the decomposition, solubilization, and polymerization of each main fraction of the biomass: cellulose, hemicellulose, and lignin. The ash content was assumed to be inert. The kinetic parameters have been obtained by non-linear adjustment using a data set with 220 experimental runs collected from the literature. The results indicate that the pre-exponential factors range was from 7.33 x10^1 to 1.412x10^5 min^{-1}, and activation energies were between 33.75 y 225.3 kJ/mol. A good fit is achieved between the observed and predicted data with an R^2 of 0.81 and an RMSE of 7.7 %. The proposed scheme was validated with the experimental data obtained by the HTC of sawdust (*Pinus radiata*) and rapeseed (*Brassica napus*). The experiments were carried out at temperatures of 190, 220, and 250 ºC and reaction times of 0, 30, 60, 90, and 120 min. The predicted values showed an average error of 2.3 and 3.5 %, respectively. Therefore, the kinetic scheme is a useful tool in the conversion analysis of waste biomass treated by HTC.

Graphical abstract

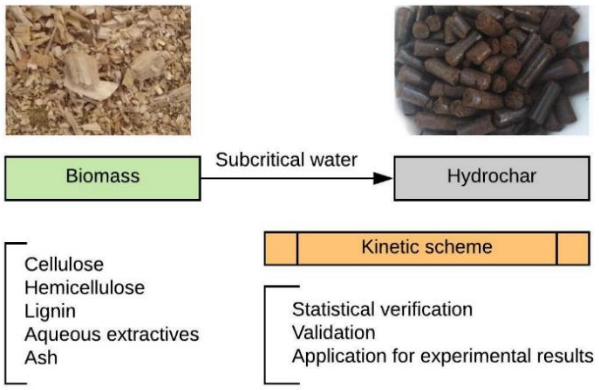

Validated kinetic scheme. A general model based on the Arrhenius equation for the decomposition of each main fraction of lignocellulosic biomass has been proposed, adjusted with literature data, validated, and applied to experimental results of residual biomass. The results show a suitable adjustment of the predicted values, with an average error of 2 - 3% and a maximum of 6%.

Keywords: hydrothermal carbonization, lignocellulosic biomass, reaction kinetic, nonlinear regression model, waste-to-energy

1. Introduction

Hydrothermal carbonization (HTC) is used for the waste biomass conversion into a solid product (hydrochar), obtaining an increase in the carbon content [1] and the higher calorific value [2]. Prior studies have shown other advantages of hydrochar, such as hydrophobic properties [3] and a lower ash content [4]. Currently, the hydrochar is used as a biofuel in boilers and stoves [5], as a precursor of activated carbon [6], catalysts [7], capacitors, among others [8,9]. The HTC has been deeply studied in some key areas, such as maximize the energy yield by analyzing the influence of the operating parameters and type of biomass treated [10–13] and the study of elemental and complex kinetics for specific biomasses [14–17]. Besides, economic and feasibility analysis have been carried out to scale the process in batch and continuous pilot plants [18–20] and to evaluate the environmental impact [21]. However, the process must overcome a few challenges as high costs of process equipment, mainly the reactor, due to inadequate knowledge of the reaction mechanism and biomass kinetic during carbonization [19].

Several previous works have studied HTC kinetic and reaction mechanisms making specific assumptions for each biomass. Therefore, the results are only applicable in limited cases since this model was not compared with others nor applied to different raw biomass. Knezevic et al. (2009) analyzed HTC of pure glucose and then extrapolated the results to two other lignocellulosic biomasses. One of the main findings was that there were no significant changes in the H/C and O/C ratios after 5 minutes of residence, with a significant decrease in the hydrogen and oxygen contents [22,23]. This reduction generates an increase in the hydrochar calorific value as oxygen content is higher than in other solid fuels. Higher heating value (HHV) of the final product reaches 30 - 33 MJ/kg, while the raw biomass HHV is between 18.5 - 21 MJ/kg [22,24,25]. Another issue to evaluate is the significant presence of volatile matter (70 – 85 %) in biomass, a higher value than traditional coal (35 – 50 %); consequently, biomass is more reactive [24]. On the other hand, the primary way to eliminate the amount of oxygen present

Peer-reviewed version available at Biofuels 2020; doi:10.1080/17597269.2020.1759179

in biomass is due to two exothermic reactions: dehydration and decarboxylation [26,27]. An increase in reaction time causes the biomass to move along the paths of these reactions in all cases considered [28].

Some studies have been developed to get a valid model to describe the biomass conversion in hydrochar evaluating mass yield (MY) and HHV, mainly linear regression models [12,13,29]. On the other hand, there is no general kinetic model for biomass available from the literature. Most studies in the field of HTC kinetic have only focused on elemental composition, i. e., carbon, oxygen, hydrogen, and nitrogen. However, some researchers have drawn attention to the very different behavior of elemental atoms (CHONS) inside of the biomass due to chemical and structural effects between lignin with cellulose and hemicellulose [15,30,31]. Therefore, this study aims to find a general kinetic scheme to describe the biomass changes during the HTC process as a function of the main fractions, i. e., cellulose, hemicellulose, and lignin. The data indicate a wide variety of biomass composition, as shown in **Table 1**.

Here: Table 1

In the same way, **Table 2** shows a summary of the main kinetic parameters for the lignocellulosic biomass fractions. It has been reported that at 200 °C, water degrades hemicellulose in furfurans and other compounds [32]. According to the study by Reza et al. (2013) [17] that evaluated the HTC process with different biomasses, there was no evidence that hemicellulose exists in the product at temperatures above 230 ºC. On the other hand, cellulose requires more energetic conditions to break the glycosidic bonds, usually acidified medium and high temperatures [17]. Cellulose degrades into oligomers, a part of them is hydrolyzed to form glucose, and the rest remains as an interlaced polymer [30]. The findings of this study indicated that at 200 °C, there was an increase in the amount of cellulose due to the elimination of

Peer-reviewed version available at *Biofuels* **2020**; doi:10.1080/17597269.2020.1759179

hemicellulose with values above 90 % at 34,5 MPa and 200 – 230 °C. Although the lignin fraction solubilization started at 200 °C, there was no significant degradation until the temperature reaches 260 -280 °C, causing a net increment of lignin content, which in some cases such as *Pinus radiata* was about three times the initial value [24,27,30].

Here: Table 2

Finally, the activation energies of hemicellulose degradation are between 82 - 156 kJ/mol for several studied cases in a temperature range of 145 - 190 °C considering first-order reactions [33]. Cellulose shows first-order kinetics in the degradation of cotton cellulose (a natural compound with the highest amount cellulose) with an activation energy of 129 kJ/mol at temperatures of 215 - 274 °C [34,35]. Other authors have found a value of 215 kJ/mol at 210 - 370 °C. Although the lignin content is usually assumed as inert, some authors did not use this assumption [36]. The studies have been developed mainly for temperatures much higher than the nominal range of HTC (180 – 280 ºC), as in the study by Zhang et al. (2007) that determined activation energies of 37 - 46 kJ/mol at 300 – 374 °C [25].

2. Methods

2.1. Data collection

This study was conducted by data collection from literature to obtain the kinetic parameters for the proposed reaction scheme by nonlinear regression and its validation with experimental runs for two Chilean lignocellulosic biomasses. The first part was carried out with a set of 220 experimental runs, about 50 lignocellulosic biomasses, recollected from the literature. The proposed kinetic scheme for this work is indicated in **Figure 1**. Aqueous extractives (AE) and hemicellulose (H) generate only soluble products, while cellulose (C) and lignin (L)

Peer-reviewed version available at Biofuels 2020; doi:10.1080/17597269.2020.1759179

decomposition produce a soluble part (liquid and gas phases) and a solid by polymerization [17,37].

Here: Figure 1

The reaction of each biomass fraction was described in the kinetic and differential form. The solution was determined by integration of the differential equations with an initial mass at time zero. It was assumed that AE goes out of the biomass completely at a temperature above 180 ° C, and all reactions were first-order, as shown in **Table 3**.

The parameters k_0, k_1, k_2, k_3, k_4, and k_5, are the first-order kinetic constants. $X_A(t)$ and A_0 are the ash contents at any time and initial time in the hydrochar, respectively. The pre-exponential factor and activation energy were determined for each constant by the Arrhenius relation, as shown in Equation 1.

$$k_i = A_i e^{\frac{-EA_i}{RT}}, for\ i = 1,2, \ldots ,5 \qquad (1)$$

R Software (*nlm* and *faraway* packages) [38,39] and Excel VBA were used to solve the equation system. The graphics were obtained by *ggplot2* [40]

Here: Table 3

2.2. Hydrothermal Carbonization

HTC experiments were carried out to evaluate the model performance. Radiata pine sawdust (AS) and rapeseed (RPS) were collected in southern Chile during the year 2018, and they were stored and used as received in the experiments. Moisture (M) was determined with the

Peer-reviewed version available at Biofuels 2020; doi:10.1080/17597269.2020.1759179

gravimetric method [41], and HHV was carried out in a Parr 6200 calorimeter (Parr Instruments, USA). Proximate analysis was performed by the Van Soest method [11] of NDF-ADF-ADL (neutral detergent fiber, acid detergent fiber, and acid detergent lignin), where the components calculated were the ash, lignin, cellulose, hemicellulose and aqueous extractives (A, L, C, H, and AE, respectively). Finally, C, O, H, and N mass fractions of AS and RPS were analyzed. **Table 4** shows the results.

Here: Table 4

Hydrothermal carbonization experiments were performed in a high-pressure reactor, model HiPR-SF5L, with a volume capacity of 5 L. The detailed description of the process can be found in previous works of this research group [3,11]. For the kinetic study, fifteen experimental runs for each biomass were carried out with a biomass – water ratio (B/W) equal to 0.10. A dry biomass amount of 300 g in each experiment was used. The temperatures analyzed were 190, 220, and 250 ºC with five reaction times: 0, 30, 60, 90, and 120 min.

3. Results and discussion

3.1. Kinetic parameters determination

A routine was developed in Excel VBA and R-Project 3.5.3 for the determination of the kinetic parameters that generated the best fit for the experimental data, measured with the Root Mean Squared Error (RMSE) and the coefficient of determination (R^2). The set of initial values were taken from the literature [17,37]. The values of each constant are indicated in **Table 5**. Although the model and the assumptions used prevent the direct comparison of values obtained with other models, the order of magnitude of the activation energies, between 33.75 to 225.3 kJ/mol, was like values reported by Reza et al. (2013): 29 and 77 kJ/mol for hemicellulose and cellulose, respectively [17]. On the other hand, the pre-exponential factors were in the same order of magnitude than parameters obtained by schemes applied to wood pyrolysis [37]. The Activation Energies reported in previous studies were higher than for this investigation, this difference can be explained by an increase in biomass reactivity due to the solubilization of the aqueous extractives fraction in the bulk liquid, and the decrease in pH generated in the early stages of the reaction [30]. The main difference found was the activation energy of lignin, which, according to this proposed scheme, was higher than that determined by Zhang et al. (2007), probably because the very different temperature range considered [25]. Besides, the activation energy for hemicellulose reaction (EA_1) was much lower than the activation energy of cellulose (EA_2, EA_3) and lignin reactions (EA_4, EA_5), because hemicellulose requires a lower process temperature to complete solubilization, i. e., its decomposition was reached faster. Several studies carried out with TGA have shown the order of decomposition of the biomass components when the reaction temperature increases: hemicellulose – cellulose – lignin [3]. While the physical significance of Arrhenius constants for heterogeneous reactions has not been clearly defined, comparing the order of magnitude of activation energies suggests that the model is consistent with the actual process and with the observations made in some studies [17,24].

Here: Table 5

The comparison between predicted and observed values indicated an R^2 of 0.81 with an RMSE of 7.7 %, as shown in **Figure 2 A**. In the same way, the residuals presented a normal distribution by applying the Shapiro Test. A p-value of 0.49 implies that the null hypothesis cannot be rejected. The standardized residuals against the theoretical quantiles are presented in **Figure 2 B**. Therefore, the proposed kinetic scheme shows a good fit and explains the decomposition of the initial solid during the process and its transformation into hydrochar.

Here: Figure 2

3.2. Case studies results

The results of sawdust HTC showed that at 190 ° C, the MY decreases from 98.7 % for a reaction time of 0 min, to 74.8 % for 120 minutes. This difference was due to the AE initial (AE_0) was solubilized ($AS\text{-}AE_0 = 2.79$ %), and there was a partial degradation of hemicellulose ($H_0 = 25$ %), which increased with the reaction time. At 220 ° C, MY changed from 77.9 to 70.6 % between 0 and 120 min, respectively, due to the partial conversion of cellulose ($C_0 = 42$ %) into hydrochar. Something similar can be observed for 250 ºC, with values between 66.5 and 55.3 %.

On the other hand, RPS had a different composition, with lower initial cellulose and lignin content, 23 and 15 %, respectively, and a higher fraction of aqueous extractives (44.6 %). At 190 °C, the values were between 59.7 and 42.2 % for 0 and 120 min, respectively, while at 250 °C, the MY obtained for 120 min was 36.5 %. As **Table 6** shows, the model developed performance in this work for both Chilean biomasses indicates a good fit for the predicted values with an R^2 of 0.81 with an RMSE of 4.3 %.

Here: Table 6

As proposed in the kinetic scheme, the AE fraction is wholly removed from the raw biomass above 180 ºC. Indeed, under the same conditions of temperature and time, the mass yield of the sawdust was higher than the rapeseed due to the difference in the AE content: AS, 2.79 %, and RPS, 44.6 %. Furthermore, sawdust has a higher lignin content, which starts to react above 260 ºC, a higher value than the range studied. Consequently, the MY average for the RPS was significantly lower.

On the other hand, no significant differences were found between the R^2 and RMSE showed in the previous subsection (0.81 and 4.3 %, respectively) and the reported values by earlier studies with models to predict MY in specific biomasses [14,42] and blends [11]. Indeed, the equations for MY obtained by Multiple Linear Regression and Regression Trees [13] indicated an R^2 of 0.85 and an RMSE of 6 %. The proposed kinetic model presented an average error with the validation data set of 2.3 and 3.5 % for sawdust and raps, respectively. The experimental values obtained for the mass yield were similar to those reported in the literature [10,11,17], allowing to validate the direct correlation between the macromolecular composition and the behavior of the biomass during the HTC process.

4. Conclusions

This work presents a novel kinetic scheme to describe the behavior of lignocellulosic biomass during the Hydrothermal Carbonization (HTC) process. The kinetic parameters were determined by a non-linear regression for Arrhenius reactions with 220 experimental runs collected from the literature. Although a direct comparison for the values obtained for the kinetic constants was not possible, an agreement in the order of magnitude was shown with models that describe the pyrolysis of lignocellulosic biomasses. The predicted values showed a determination coefficient (R^2) of 0.81 with an RMSE of 7.7 %. Finally, the model developed was applied to experimental results, showing an average error of 2.3 and 3.5 % for sawdust and rapeseed, respectively, with a maximum value of 6 % for both biomasses. These results underlined the importance of studying the macromolecular composition to predict the MY during the HTC process. A direct implication of the results obtained is the need to consider in-depth the decomposition reactions of cellulose and hemicellulose. Both fractions are removed from the raw biomass in the temperature range of 180 to 250 ºC.

Declaration of interest statement
The authors declare that they have no conflicts of interest

References

[1] M. Volpe, J. L. Goldfarb, L. Fiori, *Bioresour. Technol.* **2018**, *247*, 310–318.

[2] I. Oliveira, D. Blöhse, H.-G. Ramke, *Bioresour. Technol.* **2013**, *142*, 138–146.

[3] E. Monedero, M. Lapuerta, A. Pazo, L. A. Díaz-Robles, E. Pino-Cortés, V. Campos, F. Vallejo, F. Cubillos, J. Gómez, *Biomass and Bioenergy* **2019**, *130*, 105387.

[4] A. M. Smith, S. Singh, A. B. Ross, *Fuel* **2016**, *169*, 135–145.

[5] M. Shirai, M. Osada, A. Yamaguchi, N. Hiyoshi, O. Sato, *Recent Advances in Thermo-Chemical Conversion of Biomass*, **2015**.

[6] B. Zhang, M. Heidari, B. Regmi, S. Salaudeen, P. Arku, M. Thimmannagari, A. Dutta, *Energies* **2018**, *11*, 2022–2035.

[7] F. Safari, N. Javani, Z. Yumurtaci, *Int. J. Hydrogen Energy* **2018**, DOI 10.1016/j.ijhydene.2017.05.102.

[8] A. Jain, R. Balasubramanian, M. P. Srinivasan, *Chem. Eng. J.* **2016**, *283*, 789–805.

[9] S. Zhang, X. Zhu, S. Zhou, H. Shang, J. Luo, D. C. W. Tsang, in *Biochar from Biomass Waste*, **2019**.

[10] J. G. Lynam, M. T. Reza, W. Yan, V. R. Vásquez, C. J. Coronella, *Biomass Convers. Biorefinery* **2015**, *5*, 173–181.

[11] F. Vallejo, L. A. Diaz-Robles, F. Cubillos, R. Vega, E. Pino-Cortés, S. Carrasco, J. Gomez, *Chem. Eng. Trans.* **2019**, *76*, 1453–1458.

[12] L. Li, J. R. V. Flora, J. M. Caicedo, N. D. Berge, *Bioresour. Technol.* **2015**, *187*, 263–274.

[13] F. Vallejo, L. A. Diaz-Robles, R. Vega, F. Cubillos, *J. Energy Inst.* **2020**.

[14] D. Basso, E. Weiss-Hortala, F. Patuzzi, M. Baratieri, L. Fiori, *Energies* **2018**, *11*, 1379.

[15] D. Jung, A. Kruse, *J. Anal. Appl. Pyrolysis* **2017**, *127*, 286–291.

[16] M. Lucian, G. Piro, L. Fiori, *Chem. Eng. Trans.* **2018**, *65*, 379–384.

[17] M. T. Reza, W. Yan, M. H. Uddin, J. G. Lynam, S. K. Hoekman, C. J. Coronella, V. R. Vásquez, *Bioresour. Technol.* **2013**, *139*, 161–169.

[18] S. K. Hoekman, A. Broch, L. Felix, W. Farthing, *Energy Convers. Manag.* **2017**, *134*, 247–259.

[19] M. Lucian, L. Fiori, *Energies* **2017**, *10*, 211–215.

[20] P. McKendry, *Bioresour. Technol.* **2002**, *83*, 47–54.

[21] V. Benavente, A. Fullana, N. D. Berge, *J. Clean. Prod.* **2017**, *142*, 2637–2648.

[22] D. Knežević, W. P. M. van Swaaij, S. R. A. Kersten, *Ind. Eng. Chem. Res.* **2009**, *48*, 4731–4743.

[23] D. Knežević, W. van Swaaij, S. Kersten, *Ind. Eng. Chem. Res.* **2010**, *49*, 104–112.

[24] A. Y. Krylova, V. M. Zaitchenko, *Solid Fuel Chem.* **2018**, *52*, 91–103.

[25] R. Zhang, H. M. El-Mashad, K. Hartman, F. Wang, G. Liu, C. Choate, P. Gamble, *Bioresour. Technol.* **2007**, *98*, 929–935.

[26] A. Funke, F. Ziegler, *Biofuels, Bioprod. Biorefining* **2010**, *4*, 160–177.

[27] A. A. Peterson, F. Vogel, R. P. Lachance, M. Fröling, M. J. Antal, Jr., J. W. Tester, *Energy Environ. Sci.* **2008**, *1*, 32.

[28] X. Lu, N. D. Berge, *Bioresour. Technol.* **2014**, *166*, 120–131.

[29] K. S. Ro, J. R. V. Flora, S. Bae, J. A. Libra, N. D. Berge, A. Álvarez-Murillo, L. Li, *ACS Sustain. Chem. Eng.* **2017**, *5*, 7317–7324.

[30] T. Wang, Y. Zhai, Y. Zhu, C. Li, G. Zeng, *Renew. Sustain. Energy Rev.* **2018**, *90*, 223–247.

[31] M. Toufiq Reza, B. Wirth, U. Lüder, M. Werner, *Bioresour. Technol.* **2014**, *169*, 352–361.

[32] K. Tekin, S. Karagöz, S. Bektaş, *Renew. Sustain. Energy Rev.* **2014**, *40*, 673–687.

[33] G. Garrote, H. Domínguez, J. C. Parajó, *Holz als Roh- und Werkst.* **1999**, *57*, 191–202.

Peer-reviewed version available at *Biofuels* **2020**; doi:10.1080/17597269.2020.1759179

[34] O. Bobleter, *Prog. Polym. Sci.* **1994**, *19*, 797–841.
[35] W. Schwald, O. Bobleter, *J. Carbohydr. Chem.* **1989**, *8*, 565–578.
[36] M. Jatzwauck, A. Schumpe, *Biomass and Bioenergy* **2015**, *75*, 94–100.
[37] P. Ahuja, S. Kumar, P. C. Singh, *Chem. Eng. Technol.* **1996**, *19*, 272–282.
[38] R Core Team, **2019**.
[39] J. Faraway, *Linear Models with R*, CRC Press, Boca Raton, **2014**.
[40] H. Wickham, *Ggplot2: Elegant Graphics for Data Analysis*, Springer-Verlag, New York, USA, **2016**.
[41] International Organization for Standardization, *Solid Biofuels. Determination of Moisture Content. Oven Dry Method. Part 2: Total Moisture. Simplified Method*, **2017**, UNE-EN ISO 18134-2.
[42] E. Sabio, A. Álvarez-Murillo, S. Román, B. Ledesma, *Waste Manag.* **2016**, *47*, 122–132.
[43] E. Dinjus, A. Kruse, N. Tröger, *Chem. Eng. Technol.* **2011**, *34*, 2037–2043.
[44] S. Kieseler, Y. Neubauer, N. Zobel, *Energy and Fuels* **2013**, *27*, 908–918.
[45] J. Mumme, L. Eckervogt, J. Pielert, M. Diakité, F. Rupp, J. Kern, *Bioresour. Technol.* **2011**, *102*, 9255–9260.
[46] T. Adschiri, S. Hirose, R. Malaluan, K. Arai, *J. Chem. Eng. JAPAN* **1993**, *26*, 676–680.
[47] K. Mochidzuki, A. Sakoda, M. Suzuki, *Thermochim. Acta* **2000**, *348*, 69–76.
[48] M. Sasaki, T. Adschiri, K. Arai, *AIChE J.* **2004**, *50*, 192–202.
[49] Mitsuru Sasaki, Zhen Fang, Yoshiko Fukushima, T. Adschiri, K. Arai, *Ind. Eng. Chem. Res* **2000**, *39*, 2883–2890.

Peer-reviewed version available at *Biofuels* **2020**; doi:10.1080/17597269.2020.1759179

Table 1. Composition of various lignocellulosic biomass

Biomass	Cellulose	Hemicellulose	Lignin	Ref
Eucalyptus viminalis	41.7	14.1	31.0	[27]
Oak	40.4	35.9	24.1	[27]
Pinus radiata	42 – 50	24 – 27	20	[27]
Corncob	33.7 – 41.2	31.9 – 36	6.1 – 15.9	[27]
Wheat straw	32.9 – 50	24 – 33.5	8.9 – 17.3	[27]
Rice straw	36.2 – 47	19 – 24.5	9.9 – 24	[27]
Vine sprouts	35.6 – 38.3	20.6 – 35.0	22.8 – 23.4	[27]
Cauliflower	70.0	11.0	10.0	[43]
Grass	45.0	41.0	4.0	[43]
Beechwood	59.0	22.0	18.0	[43]
Wheat stalk	40.0	28.0	17.0	[44]
Digestate maize silage	26.0	1.0	38.0	[45]

Table 2. Kinetic parameters for main biomass fractions

Fraction[a]	Temperature (ºC)	Reaction order	Activation energy (kJ/mol)	Biomass	Ref
	215 – 274	Arrhenius, first-order	129.1	Cotton	[35]
	250 – 320	Arrhenius, first-order	165	Cellulose	[46]
C	198 – 262	Arrhenius, first-order	220	Cellulose	[47]
	300 - 400	Arrhenius, first-order	146 – 548	Microcrystalline cellulose	[48,49]
	210 – 370	Data fit by regression	215	Various	[27]
H	145 – 190	Arrhenius, first-order	82 – 156	Various	[33]
L	300 – 374	Arrhenius, first-order	37 – 46	Pure lignin and oatmeal hulls	[25]

(a) C: Cellulose, H: Hemicellulose, L: Lignin

Table 3. Scheme kinetic for biomass fractions

Biomass fraction	**Kinetic reaction**	**Differential equation**	**Solution**
Aqueous extractives	$AE \rightarrow W$	$\frac{dAE}{dt} = -k_0[AE]$	$X_{AE}(t) = 0, T > 180\ ºC$
Hemicellulose	$H \rightarrow W$	$\frac{dH}{dt} = -k_1[H]$	$X_H(t) = H_0 e^{-k_1 t}$
Cellulose	$C \rightarrow H_C$	$\frac{dC}{dt} = -(k_2 + k_3)[C]$	$X_{H_C}(t) = C_0 \frac{k_2}{k_2 + k_3} e^{-(k_2+k_3)t}$
	$C \rightarrow W$		$X_C(t) = C_0 e^{-(k_2+k_3)t}$
Lignin	$L \rightarrow H_L$	$\frac{dL}{dt} = -(k_4 + k_5)[L]$	$X_{L_C}(t) = L_0 \frac{k_4}{k_4 + k_5} e^{-(k_2+k_3)t}$
	$L \rightarrow W$		$X_L(t) = L_0 e^{-(k_4+k_5)t}$
Ash			$X_A(t) = A_0$
Mass yield		$MY(t) = X_H(t) + X_{H_C}(t) + X_C(t) + X_{L_C}(t) + X_L(t) + X_A(t)$	

Table 4. Raw biomass characterization

Biomass	**M (%)**	**Proximate analysis**					**HHV (MJ/kg)**	**Ultimate analysis**			
		A (%)	L (%)	C (%)	H (%)	AE (%)		C (%)	H (%)	N (%)	O (%)
AS	7.45	0.29	30.0	42.0	25.0	2.79	19.28	48.8	6.20	0.13	44.8
RPS	7.32	7.37	15.0	23.0	10.0	44.6	21.36	49.7	6.85	5.30	30.8

Peer-reviewed version available at *Biofuels* **2020**; doi:10.1080/17597269.2020.1759179

Table 5. Kinetic parameters for proposed scheme

Biomass fraction reaction	**Pre-exponential Factor (min^{-1})**	**Activation Energy (kJ/mol)**
Hemicellulose	$A_1 = 7.71 \times 10^1$	$EA_1 = 33.78$
Cellulose	$A_2 = 1.41 \times 10^5$	$EA_2 = 83.75$
	$A_3 = 5.79 \times 10^4$	$EA_3 = 72.40$
Lignin	$A_4 = 1.62 \times 10^4$	$EA_4 = 150.1$
	$A_5 = 1.10 \times 10^4$	$EA_5 = 225.3$

Table 6. Observed and predicted mass yields for sawdust and rapeseed

T (°C)	t (min)	AS			RPS		
		MY	pred MY	error	MY	pred MY	error
190	0	98.7 %	93.1 %	5.5 %	59.7 %	53.3 %	6.3 %
	30	88.8 %	86.4 %	2.5 %	54.6 %	50.6 %	4.0 %
	60	83.6 %	81.5 %	2.1 %	52.3 %	48.5 %	3.8 %
	90	78.8 %	77.9 %	0.8 %	49.7 %	47.0 %	2.7 %
	120	76.8 %	75.3 %	1.4 %	42.2 %	45.9 %	3.7 %
220	0	77.9 %	80.6 %	2.7 %	54.7 %	48.3 %	6.4 %
	30	74.3 %	75.3 %	1.0 %	49.4 %	46.0 %	3.4 %
	60	73.2 %	71.7 %	1.5 %	47.2 %	44.3 %	2.9 %
	90	71.7 %	69.2 %	2.5 %	46.5 %	43.1 %	3.3 %
	120	70.6 %	67.3 %	3.3 %	44.2 %	42.1 %	2.1 %
250	0	66.5 %	63.9 %	2.6 %	46.4 %	40.4 %	6.0 %
	30	63.1 %	60.6 %	2.5 %	42.3 %	38.6 %	3.7 %
	60	59.3 %	57.8 %	1.5 %	38.7 %	37.1 %	1.6 %
	90	57.5 %	55.2 %	2.3 %	37.8 %	35.7 %	2.1 %
	120	55.3 %	53.0 %	2.4 %	36.5 %	34.4 %	2.1 %

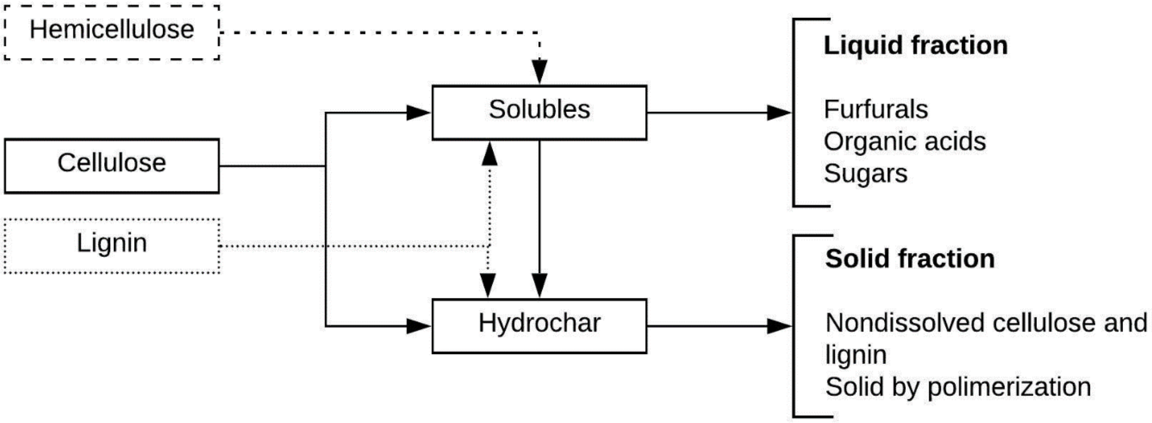

Figure 1. Kinetic scheme for biomass reactions to hydrochar

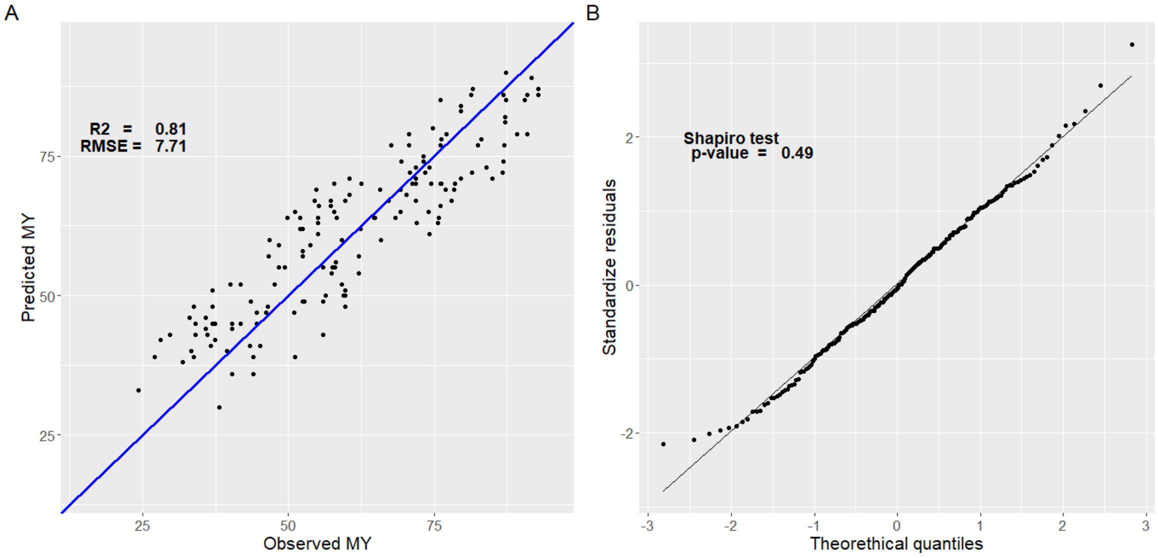

Figure 2. Observed and predicted mass yield values for the proposed kinetic model

Peer-reviewed version available at *Biofuels* **2020**; doi:10.1080/17597269.2020.1759179

Figure Captions

Figure 1. Kinetic scheme for biomass reactions to hydrochar

Figure 2. Observed and predicted mass yield values for the proposed kinetic model